PNAS Nexus

PNAS Nexus, 2022, **1**, 1–11
https://doi.org/10.1093/pnasnexus/pgac254
Advance access publication date: 4 November 2022
Research Report

Latitudinal shifts of soil microbial biomass seasonality

Fazhu Zhao[a,b,†], Liyuan He[b,*,†], Ben Bond-Lamberty[c], Ivan A. Janssens[d], Jieying Wang[a], Guowei Pang[a], Yuwei Wu[a] and Xiaofeng Xu[b,*]

[a]Shaanxi Key Laboratory of Earth Surface System and Environmental Carrying Capacity, Northwest University, Xi'an 710127, China
[b]Biology Department, San Diego State University, San Diego, CA 92182, USA
[c]Pacific Northwest National Laboratory, Joint Global Change Research Institute at the University of Maryland–College Park, College Park, MD 20740, USA
[d]Department of Biology, University of Antwerp, Universiteitsplein 1, B-2610 Wilrijk, Belgium
*To whom correspondence should be addressed: Emails: lhe2@sdsu.edu; xxu@sdsu.edu
Edited By: Christopher Dupont

Abstract

Soil microbes ultimately drive the mineralization of soil organic carbon and thus ecosystem functions. We compiled a dataset of the seasonality of microbial biomass carbon (MBC) and developed a semi-mechanistic model to map monthly MBC across the globe. MBC exhibits an equatorially symmetric seasonality between the Northern and Southern Hemispheres. In the Northern Hemisphere, MBC peaks in autumn and is minimal in spring at low latitudes (<25°N), peaks in the spring and is minimal in autumn at mid-latitudes (25°N to 50°N), while peaks in autumn and is minimal in spring at high latitudes (>50°N). This latitudinal shift of MBC seasonality is attributed to an interaction of soil temperature, soil moisture, and substrate availability. The MBC seasonality is inconsistent with patterns of heterotrophic respiration, indicating that MBC as a proxy for microbial activity is inappropriate at this resolution. This study highlights the need to explicitly represent microbial physiology in microbial models. The interactive controls of environments and substrate on microbial seasonality provide insights for better representing microbial mechanisms in simulating ecosystem functions at the seasonal scale.

Keywords: heterotrophic respiration, latitude, soil microbial biomass, seasonality

Significance Statement:

Soil microbes drive soil organic matter mineralization under the control of environmental factors. With a global dataset and a semi-mechanistic model, we developed a framework for the joint controls of temperature, moisture, and substrate on soil microbial biomass, which was further used to map the monthly soil microbial biomass across the globe. A latitudinal shift of microbial seasonality was found, which infers the divergent microbial mechanisms across the space, highlighting the need to explicitly represent microbial seasonality in global carbon models.

Introduction

Soil microbes ultimately drive the mineralization of organic carbon (C) in soils (1, 2), despite the relatively small portion (1.3% in top 1 m) in global soil organic C (SOC) (3). Higher soil microbial biomass usually leads to a faster C mineralization (4, 5). Therefore, soil microbial biomass is positively correlated with SOC mineralization, the dominant source of heterotrophic respiration (Rh) in terrestrial ecosystems (6, 7, 8). This linear and positive association has been a foundation for the assumption in many microbial models that microbial biomass is a proxy for the microbial activity of the SOC mineralization (9, 10).

This positive association between microbial biomass C (MBC) and Rh has been widely observed at the site level (4, 8). It is primarily attributed to the linear correlation between MBC and the presence of microbial enzymes for decomposing SOC (11, 12). However, this correlation does not always hold true. For instance, Wei et al. (13) documented a positive correlation between MBC and Rh in warm seasons but not in cold seasons. Other studies reported that microbial biomass is not always the limiting factor for Rh, highlighting the critical roles of substrate availability, temperature, and moisture (14, 5). A global synthesis found the inconsistent seasonal dynamics between MBC and Rh in multiple ecosystems (i.e., arable, grassland, forest, and desert shrubland) (15). This inconsistency infers our limited understanding of how MBC varies across seasons and at what timescales it is (or is not) linked to Rh.

Soil microbes and their microhabitat change over seasons, while the seasonal patterns vary among studies. For example, Díaz-Raviña et al. (16) observed higher MBC in spring and winter than in summer and autumn in four temperate coniferous forest sites and a temperate broadleaf forest site in the Northern Hemisphere. Cochran et al. (17) reported the peak MBC during June and July in forest soils of Arctic regions in the Northern Hemisphere. However, Edwards and Jefferies (18) reported the highest MBC in

Competing Interest: The authors declare no competing interest.
†F.Z. and L.H. contributed equally to this work.
Received: June 13, 2022. **Revised:** August 26, 2022. **Accepted:** November 1, 2022

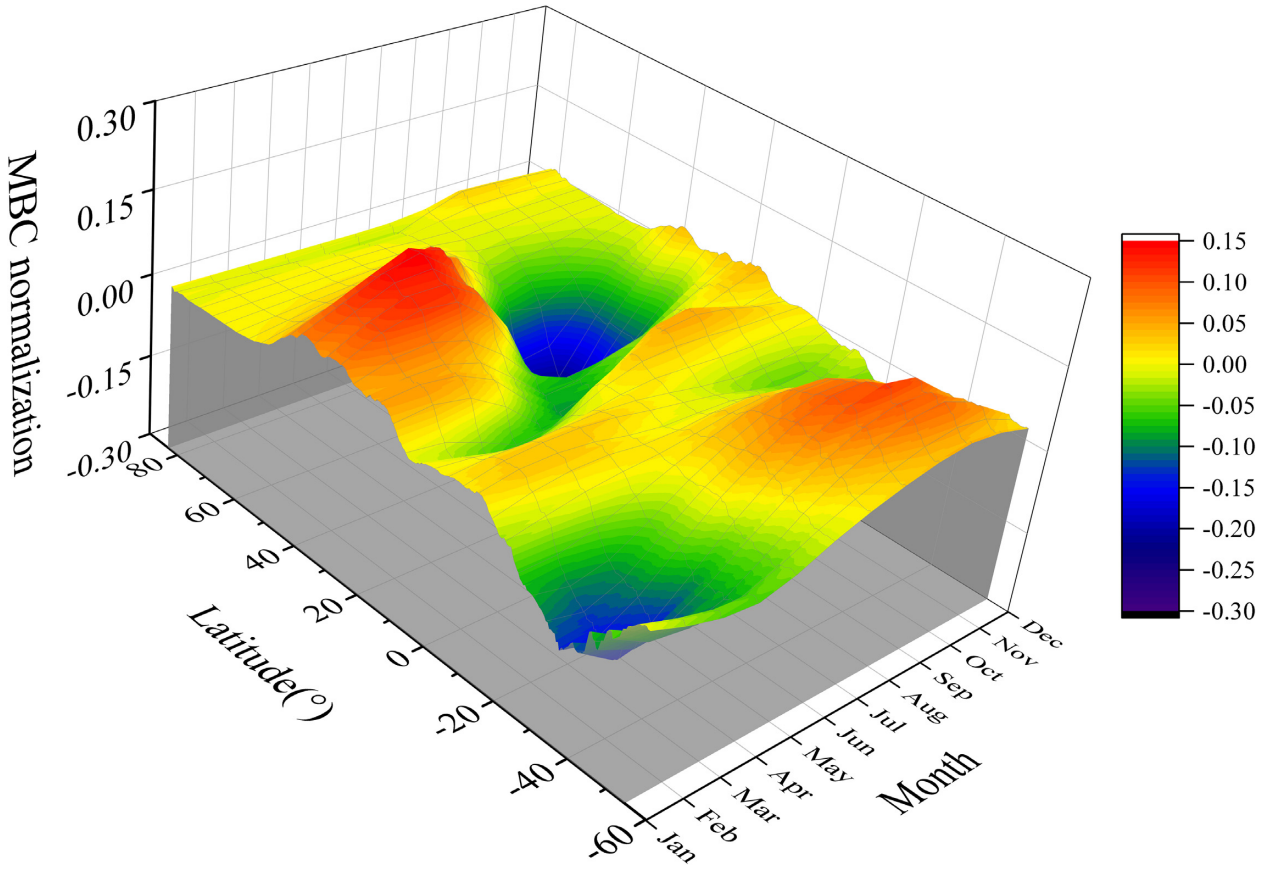

Fig. 1. Latitudinal distribution of the normalized MBC seasonality.

winter and a sharp decrease during soil thaw (spring) in wet and dry low-Arctic sedge meadows in the Northern Hemisphere. The shifting microbial seasonality might be caused by interactions of environmental factors and substrate availability; Moreover, studies reported that MBC was more strongly affected by soil temperature, soil water availability (19), and carbon inputs (20) at a seasonal scale. Therefore, a holistic understanding of the MBC seasonality and its controls remains to be investigated.

To address this gap, we compiled a global dataset of MBC seasonality, including 686 data points from 110 full-year seasonal measurements and 1204 data points from 145 nonfull-year seasonal measurements (see the "Materials and methods" section). Meanwhile, we included 2389 data points of Rh from 125 full-year seasonal measurements (see the "Materials and methods" section). Specifically, we investigated the seasonal pattern of soil MBC and its controls and examined the consistency between MBC and Rh on a monthly scale. To eliminate biases of cross-site variations in MBC, we normalized the MBC at each site and focused on the seasonal variation of MBC and its controls on a global scale. Four algorithms for data normalization were evaluated, and the logarithmic transformation was adopted due to its superiority in transforming data to ensure the normality of the data (Fig. S1, Supplementary Material).

Results

Seasonality in soil MBC and environmental factors

The monthly MBC was reproduced with a revised semi-mechanistic model (10). Fundamental microbial physiological processes such as C assimilation, decomposition, microbial growth and death, and microbial maintenance respiration were included in the semi-mechanistic model (Fig. S2, Supplementary Material). The comparisons between simulated and observed MBC yielded reasonable consistency by latitudinal zones (0°N to 25°N, 25°N to 50°N, and 50°N to 90°N) (Figs. S3 and S4, Supplementary Material), months (Fig. S5, Supplementary Material) and at the biome level (Fig. S6, Supplementary Material). The model was able to explain 77% of the variations in observational data across the sites (Fig. S7, Supplementary Material).

The modeled soil MBC exhibited a clear seasonality, but the seasonal pattern and amplitude varied with latitudes (Fig. 1, Figs. S9, S10, and S12A, Supplementary Material). The standardized modeled MBC further confirmed those trends—a strong seasonality in mid-latitudes (25°∼50°) but a relatively weak seasonal variation in low latitudes (0∼25°) and high latitudes (>50°) of the Northern and Southern Hemispheres. Specifically, in the Northern Hemisphere, MBC peaked in September and bottomed during March in low latitudes [standard deviation (SD) of the monthly standardized MBC ranged from 0.008 to 0.044], peaked in April and bottomed in September in mid-latitudes (SD: 0.009 to 0.056), and peaked in May and bottomed in October in high latitudes (SD: 0.005 to 0.045). The coefficient of variation (CV) of the MBC displayed the same pattern; the 95% CI of the CV was 0.8%∼28.2% in high latitudes, 6.6%∼40% in mid-latitudes, and 1.7%∼27.6% in low latitudes across the globe (Fig. S11, Supplementary Material). Overall, MBC exhibited an equatorially symmetric seasonality in the Northern and Southern Hemispheres (Fig. 1). The seasonal variations in soil temperature (ST), soil moisture (SM), and carbon inputs (i.e., gross primary production) are observed. The sea-

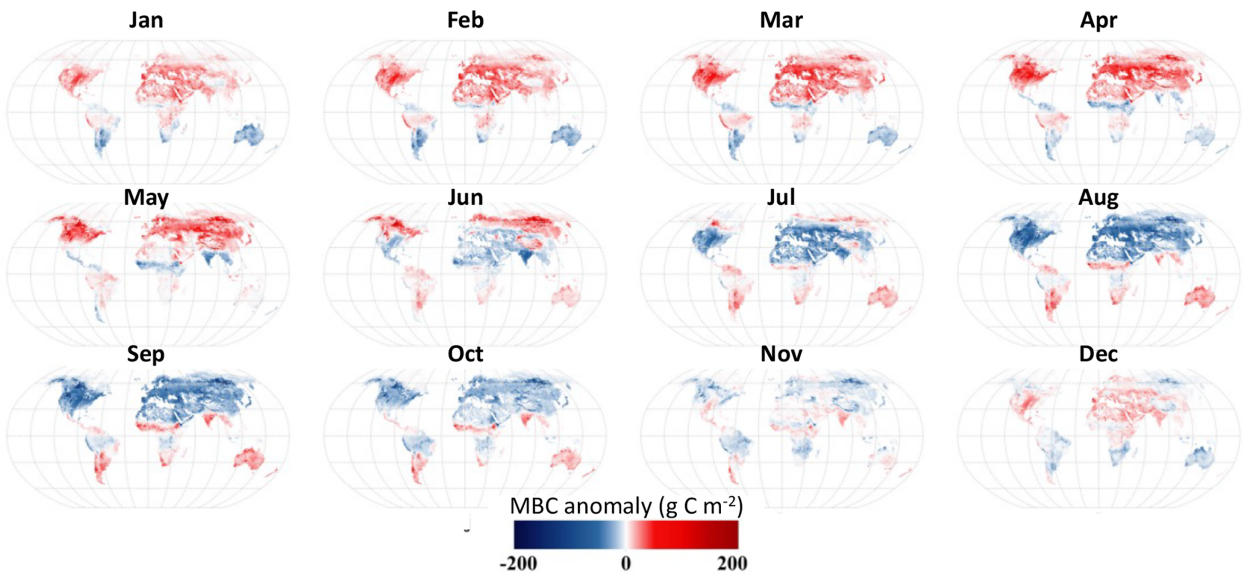

Fig. 2. Global distribution of MBC anomalies in each month (MBC anomaly was calculated with the equation MBC_i—$\overline{MBC}$; MBC_i represents MBC for the i_{th} month, $\overline{MBC}$ is the arithmetic means of monthly MBC in 1 year)

sonality of ST kept relatively consistent across the latitude in the Northern Hemisphere, peak in August, and bottom in January; the seasonality of SM showed a slight shift along latitude, with a special nadir in winter in the 15°∼20° latitudinal zone, corresponding to the large desert regions in northern Africa. The carbon input expressed as gross primary production has a clear seasonality, and it declines from low to high latitudes (Fig. S8, Supplementary Material).

Monthly soil MBC at the global scale

The MBC showed substantial variations across space and seasons (Figs. S9 and S10, Supplementary Material). Globally, the MBC declines from high to low latitudes (Figs. S9 and S10, Supplementary Material). The SD of absolute MBC remained large, ranging from 90.7 to 97.1 gC m^{-2} among months and 90.9 to 94.3 gC m^{-2} among the four seasons. To further visualize the MBC seasonality, we mapped the MBC anomaly (monthly MBC - annual mean MBC) for all 12 months (Fig. 2). The monthly MBC anomaly shows a clear shift from month to month, transitioning from positive anomalies in winter and spring months to negative anomalies in summer and fall months in the Northern Hemisphere. That seasonal trend is oppositive over the equator: the monthly MBC transitioned from negative anomalies in winter and spring months to positive anomalies in summer and fall months in the Southern Hemisphere (Fig. 2).

MBC seasonality at the biome level

Seasonal changes in MBC storage are distinct among biomes in both Northern and Southern Hemispheres (Fig. 3; Tables S3 and S4, Supplementary Material). The highest MBC storage was found in the boreal forest, pasture, tundra, cropland, desert, tropical/subtropical forest, mixed forest, grassland, shrubland, temperate coniferous forest, and natural wetlands during March to May and December to February in the Northern Hemisphere. However, we found high MBC storage during June to August across biomes except for temperate broadleaf forest, tropical/subtropical forest, mixed forest, tundra, and desert in the Southern Hemisphere. Notably, the MBC storage was higher in the temperate broadleaf forest than in tropical/subtropical forests (4.09–4.52 Pg C vs. 0.83–0.90 Pg C) during March to May, December to February, June to August, and September to November in the Northern Hemisphere. The pasture had higher MBC storage than grasslands (1.33–1.82 Pg C vs. 0.79–0.97 Pg C) during March to May, December to February, June to August, and September to November in the Northern Hemisphere. However, the MBC storage was the highest in tropical/subtropical forests in the Southern Hemisphere and was higher than in temperate broadleaf forests (0.93–1.03 Pg C vs. 0.026–0.030 Pg C) during March to May, December to February, June to August, and September to November. Meanwhile, we did not find differences in MBC storage between pasture and grassland; but they have higher MBC storage than wetlands, tundra, mixed forest, and desert in the Southern Hemisphere (Fig. 3; Table S4, Supplementary Material).

Seasonal discrepancies between MBC and Rh

We found a substantial discrepancy in seasonality between modeled MBC and Rh from multiple sources (Fig. S12, Supplementary Material). The Rh data are derived from CIMP6 (Coupled Model Intercomparison Project Phase 6), data compiled in this study, and Konings datasets (21). Seasonal patterns of MBC and Rh were contrasting for latitudes of 0°N to 25°N ($r < 0$), substantial inconsistency was observed between MBC and Rh at 0°N to 90°N and 25°S to 90°S; whereas the inconsistency was relatively weak during January to April at latitudes of 0°S to 50°S.

A conceptual diagram of MBC seasonality and its controls

We further developed a conceptual diagram to illustrate the MBC seasonality considering the interactive role of ST, SM, and substrates [C in litter and soil organic matter (SOM)] on microbial life (Fig. 4). The controls on MBC variation are implemented in four stages, corresponding to four phases of MBC seasonality (i.e., valley, phase 1; increasing, phase 2; peak, phase 3; and declining, phase 4). To better interpret variations in MBC, regions with the most distinguished four-phase pattern in low (10° to 20°), middle (40° to 50°), and high (70° to 80°) latitudes in the Northern Hemi-

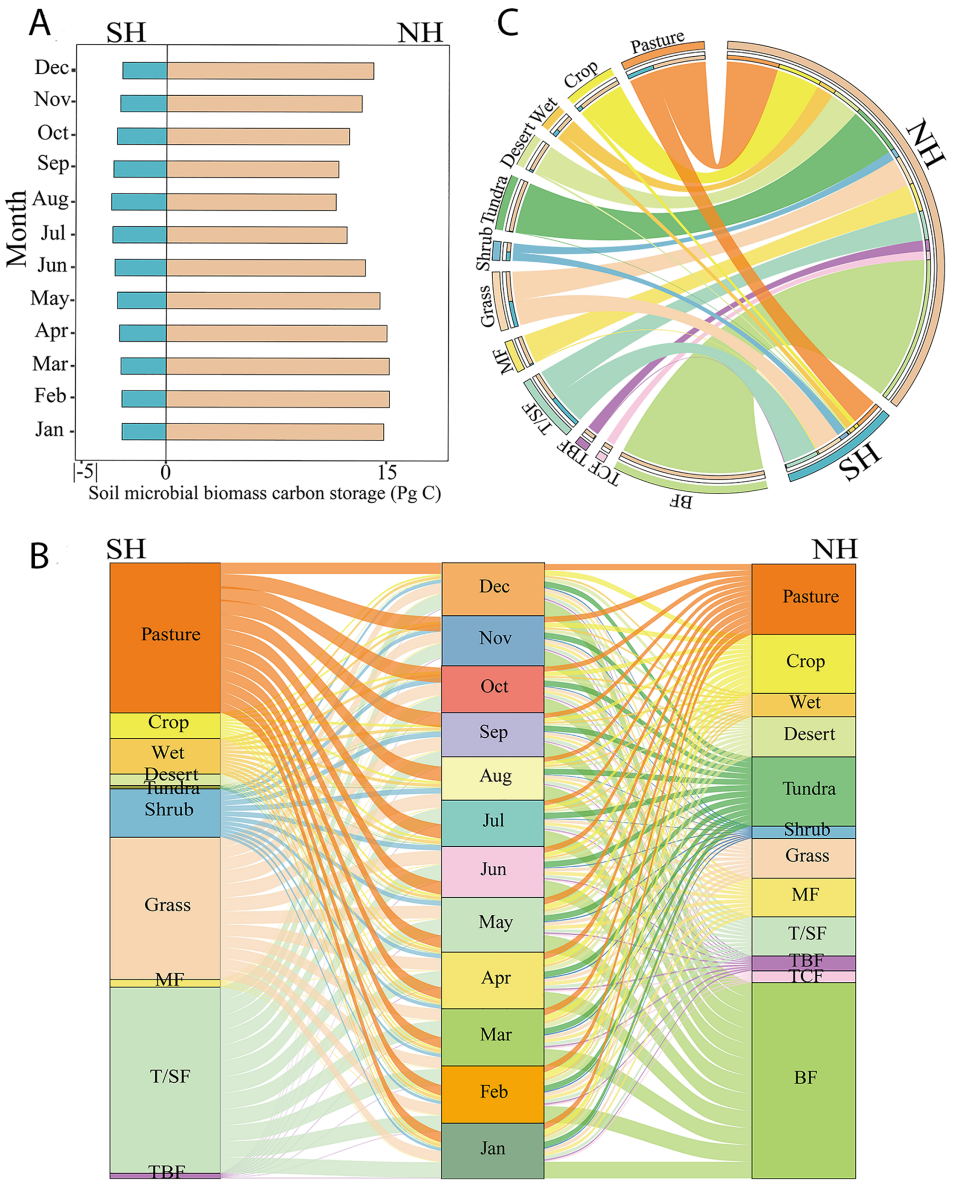

Fig. 3. Biome-level soil MBC storage (Pg C) in the Northern and Southern Hemispheres; including (A) monthly soil MBC storage in the Northern and Southern Hemispheres; (B) changes of soil MBC storage among months at the biome level; (C) biome-level soil MBC storage in the Northern and Southern Hemispheres; BF: Boreal Forest; TCF: Temperate Coniferous Forest; TBF: Temperate broadleaf forest; T/SF = Tropical/Subtropical Forest; MF: Mixed Forest; Grass: Grassland; Shrub: Shrubland; Wet: Natural wetlands; and Crop: Cropland.

sphere were included for analysis (see the "Materials and methods" section). In each latitudinal zone, 12 months were classified into four phases based on their stage of microbial seasonality (e.g., valley, increasing, peak, and declining). Finally, randomly selected 100 data pairs of substrates, ST, and SM in each phase of three latitudinal zones, 1200 data pairs in total, were included for generalized linear analysis to attribute variations in MBC. In phase 1, the interaction between substrate and SM dominated MBC, explaining 41.2% of its variation; in phase 2, the interaction between substrate and ST (38.7%) controlled MBC; in phase 3, the interaction between substrate and ST (27.2%) was the main factor affecting MBC, and in phase 4, ST (47.5%) was dominant.

Discussion

The shifting MBC seasonality along latitude is primarily caused by three mechanisms. First, microbial biomass accumulation is co-regulated by soil climate condition, pH, nutrient availability, and labile substrate degradation (22, 23, 24). For example, Lipson et al. (25) observed the lowest MBC in summer and attributed the MBC drop to warming-led degradation of labile C, leading to substrate limitation and thus a tiny MBC pool size. It can be verified in this study by the strong controls by ST, SM, and substrate (Fig. 4); specifically, when the ST and SM are not limiting factors, weak MBC seasonality forms and the large substrate availability dominates the peak of MBC in Fall season in the low latitudes (Figs. 1 and 4). Second, predators may also play an essential role in microbial biomass variations. For example, soil protozoa can depend on MBC, strongly shaping the soil MBC dynamics (11). Predators (e.g., nematodes and protozoa) have substantial impacts on the soil microbial community by regulating the size and composition of the microbial community and accelerating the turnover of the microbial biomass (26). The warmer temperature might promote nematode and protozoa that prey on microbes and lead to MBC

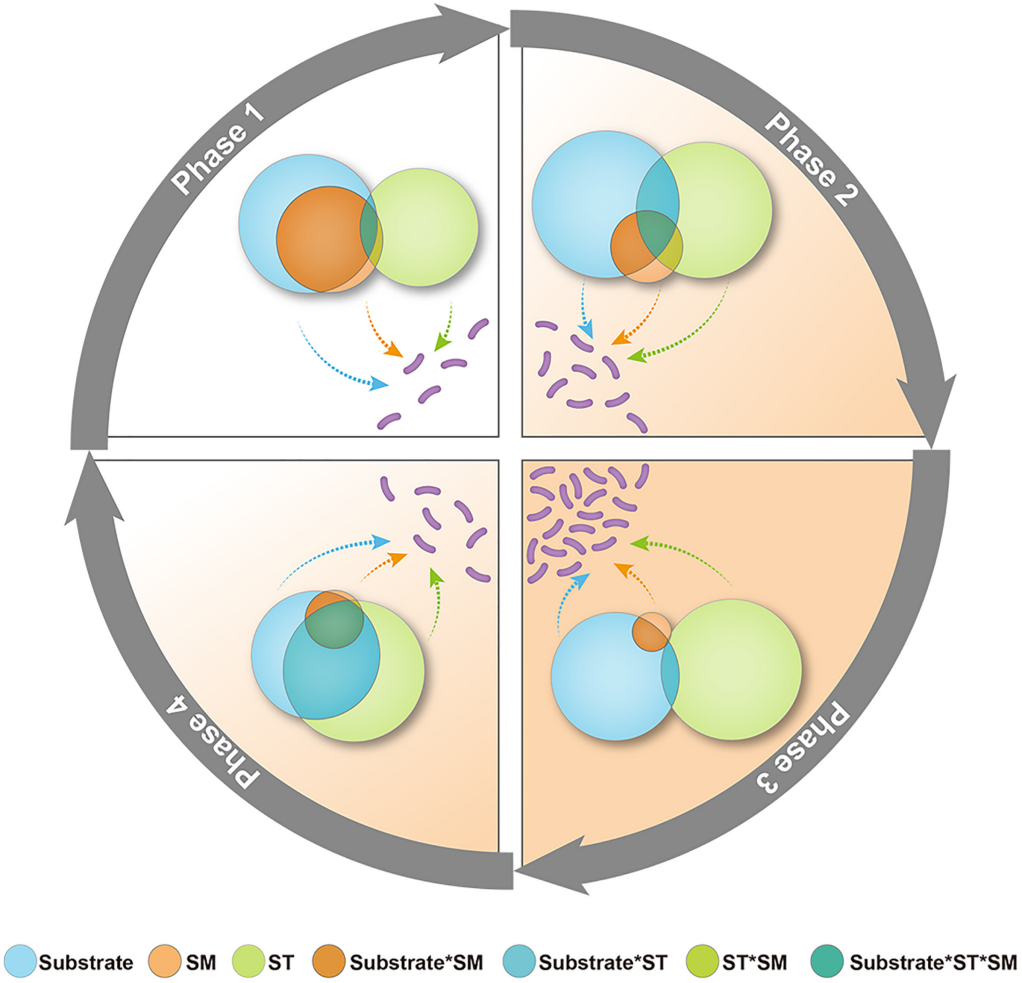

Fig. 4. Diagram illustrating the MBC seasonality regulated by substrate availability, ST, SM, and their interactions. Four phases correspond to changing stages of MBC at the seasonal scale: phase 1 represents the stage with the lowest MBC, phase 2 is the transitioning stage from the lowest to the highest MBC, phase 3 is the stage with the highest MBC, and phase 4 represents the MBC depletion stage. Green, red, and blue circles represent ST, SM, and substrate, respectively, and the overlap area represents the interactions between and among variables. The size of the circles for factorial interactions represents the strength of the contribution of factors by individual or combination. Small purple pods represent the relative abundance of microbes.

reductions (27). Lastly, the seasonal variation of MBC can result from the competition between soil microbes and plants for nutrients. Plant-microbe competition for nutrients has been reported in a range of ecosystems, such competition impacts on microbial nutrient immobilization are largely influenced by traits of plant species such as root density, rooting depth, and timing of the growing season (28, 29). The difference in plant traits across space can therefore induce the shifts of MBC seasonality along latitude.

In addition to the natural variation in environmental factors, some biotic factors such as the high diversity of plant biomes (e.g., deciduous and evergreen forests, shrubs, grass, and mixed forests) and microbial species (30) can contribute to the large seasonal variation in MBC in mid-latitudes. Plants are different in impacting soil microbes. For example, Wang et al. (31) found that both experimental results and synthesized dataset suggest higher root exudation rates and larger impacts on soil microbial change of deciduous tree species than of evergreen tree species. In addition, soil microbial species varied in response to environmental changes. Bacterial communities tend to show a greater response to changes in environmental conditions and plant communities than fungal communities (32). The variations in soil environments and high abundances of plant and microbial species may cause the large seasonal variation of soil microbes.

Biome-level differences in MBC storage were jointly determined by substrate, ST, and SM. For example, the temperature was critical in determining the temporal variability of MBC in temperate ecosystems. In contrast, peak microbial biomass was usually attributed to favorable soil moisture in tropical forests (15). The difference in C availability can be responsible for the distinct seasonal patterns of MBC among biomes (20). The C input from root growth is positively correlated with the microbial biomass (33). Thus the seasonality of root growth may drive distinct seasonal patterns of MBC among biomes (34).

Five mechanisms may explain the inconsistency between the seasonality in MBC and RH. First, soil microbial community composition shifts among seasons—for example, fungi showed significantly higher dominance over bacteria in winter than in summer in a dry alpine meadow (35). Second, the difference in substrates and microbial properties can partly explain the inconsistent seasonal pattern between MBC and Rh by latitude. The distinct microbial turnover rates (36), soil organic carbon chemical composition (37), and substrate use efficiency (38), and their differences in seasonal variations can partly explain the discrepancy between MBC and Rh along latitude. Third, vegetation labile C input plays an important role in determining the inconsistent seasonal patterns between MBC and Rh. Labile C is a critical source

of microbial biomass accumulation, which tends to have higher microbial carbon use efficiency (CUE). The seasonal variations of vegetation labile C input may be tightly associated with the MBC seasonality (39, 40). The CUE, co-regulated by enzymatic activity and microbial community properties, is the tradeoff between microbial biomass and respiration. Increasing microbial CUE corresponds to reductions in the microbial respiration (41). The CUE showed a broad range (0.1 to 0.6) (42), which inevitably results in MBC and microbial respiration asynchrony (41). Fourth, the time lag between microbial respiration activities and biomass assimilation can explain the inconsistent seasonality between MBC and Rh. In addition to biomass synthesis, microbes spend energy on synthesizing components for microbial growth such as enzyme production. The microbes may exhibit enhanced microbial respiration activity for synthesizing components essential for microbial growth rather than biomass, leading to the time lag between Rh and MBC (43). Finally, different responses of microbial biomass maintenance and respiration to environmental change may account for the inconsistent seasonality between MBC and Rh. For example, microbial turnover and respiration are temperature-sensitive; both are enhanced by rising temperature (36, 44, 45). Although soil microbes are major drivers of Rh, the tradeoff between soil microbial biomass maintenance and respiration can partially explain the seasonal inconsistency between MBC and Rh.

The inconsistency between MBC and Rh at a seasonal scale indicates that microbial physiology may play a predominant role in affecting the SOC mineralization (46, 47). The inconsistency between MBC and Rh also challenges the traditional view that declining microbial biomass leads to a possible decline in Rh (48, 49). A complete model representation of microbial biomass, community structure, and microbial activities is thus needed for better projecting microbial roles in global C cycling.

There are a few limitations of the current study that will be addressed in future work. First, various methods have been used to quantify MBC and Rh, which may bias MBC and Rh measurements. Multiple techniques including fumigation extraction (FE), substrate-induced respiration (SIR), phospholipid fatty-acid analysis (PLFA), and fluorescein diacetate-active (FDA), were used in MBC measurements, while root trenching, root removal, and gap analysis were utilized for Rh estimation. Differences in assessment techniques can cause biases in the cross-site comparison (50, 51, 3). Second, inconsistencies in sampling timing and frequency among sites might be another source of MBC fluctuation. The data proportion for each month is not uniform throughout the year; for example, the data point was as high as 13.4% for April and as low as 5.2% for June. The disproportional sources of data and their spatial representation might cause bias in MBC extrapolation to a global scale; specifically, approximately 70% of data points were obtained from Asia, 12.3% of data were from America, and 16.1% of data were taken in Europe. Furthermore, all data points were obtained in the Northern Hemisphere, and no data were available from the Southern Hemisphere. We thus call for field campaigns on monthly microbial properties in underrepresented areas (52). Last but not the least, despite the mechanistic representation of ST, SM, and substrate (mainly litter and SOM) in the model, other factors, including predators, pH, and root exudates, may be necessary for the MBC estimation [e.g., Kooch and Noghre (27)], which deserves further mechanistic analysis.

This study represents the first attempt to investigate the seasonality of MBC and produces global maps of monthly MBC. These data are valuable for better understanding the land-climate feedback, as seasonal fluctuations of MBC associated with microbial decomposition play an essential role in terrestrial C and nutrient cycles (15). The mineralization of SOM by soil microbes provides nutrients for plant growth, and the release of nutrients during decomposition is highly dependent on the stoichiometric ratio of substrate and microbial biomass. Soil microbes can essentially maintain element homeostasis; dynamics in MBC can, therefore strongly affect nutrient availability for plants (53).

Materials and methods

This study was carried out in four steps. First, we compiled a comprehensive dataset of MBC and Rh by searching peer-reviewed publications and from other published datasets. Second, we analyzed the seasonal patterns of MBC in multiple latitudinal zones, and a semi-mechanistic model was applied to reproduce the seasonality of microbial biomass. Third, combining the relative change in monthly MBC from the semi-mechanistic model and the global map of MBC, we produced a monthly global map of MBC. Fourth, a generalized linear model was applied to quantify the contributions of the substrate and environmental factors (e.g., ST and SM) to the seasonal variations of MBC.

Data compilation

We used Google Scholar (http://scholar.google.com/) for a comprehensive search of peer-reviewed papers published by December 2020. We searched using the keyword combination of (a) "seasonal change" or "seasonal variation" or "seasonal dynamics" or "monthly variation" or "seasonality" and (b) "microbial biomass," or "fungi biomass," or "bacterial biomass," or "microbial activity," or "enzyme," and (c) "soil" or "land."

We screened papers with seasonal variations of MBC based on five criteria. First, we only included studies measuring MBC in all seasons (i.e., spring, summer, autumn, and winter) and taking at least one measurement in each season into the dataset. In this study, we defined December to February as winter, March to May as spring, June to August as summer, and September to November as autumn in the Northern Hemisphere, while we defined December to February as summer, March to May as autumn, June to August as winter, and September to November as spring in the Southern Hemisphere. Second, if studies included part of a season in one year but the other seasons in the next year, we used the corresponding months in the next year to supplement the data. For example, if a study measured MBC in months 9 to 12 in 2000 and months 1 to 7 in 2001, then we assumed that these measurements represented the soil MBC for an entire year. Third, if a study reported spring, summer, autumn, and winter in one year but without any clear information of the sampling month, we assumed that the sampling was done in the middle of each season, i.e., April, July, October, and January, respectively, in the Northern Hemisphere. Fourth, details on soil microbial biomass measurement methods had to be provided in each publication. Finally, soils for microbial biomass measurements were taken from natural conditions or control plots of 0 to 20 cm soil depth in the field.

Eventually, we included 110 full-year seasonal variation measurements with 686 full-year data points from 53 articles, 145 nonfull-year seasonal variation measurements with 542 nonfull-year data points from 64 articles, and 662 nonfull-year data points from NEON into our dataset for the model validation (Dataset and Table S1, Supplementary Material). Available associated information, such as the sampling site, sampling depth, sampling date, latitude, longitude, mean annual precipitation, and mean annual temperature, was also recorded into the dataset. For data points without geographical coordinates reported in the literature, we

searched their geographical coordinates based on the names of site, state, and country.

Five different methods—FE, SIR, PLFA, and FDA—were used to measure soil MBC, with FE measurements accounted for 72.6%, SIR measurements accounted for 13.5%, PLFA measurements accounted for 9.8%, and FDA measurements accounted for 4.0% of the datapoints in the dataset. All measurements of soil MBC were converted to the unit of mg kg^{-1}. To normalize the data, we performed log- (a), max- (b), mean- (c), and square root- (d) transformations for MBC (frequency distributions are shown in the Supplementary Material). We chose the log_{10} transformed value of MBC for subsequent data analysis due to its better normal distribution.

To locate papers reporting Rh, we used the keyword combinations such as "microbial respiration" or "heterotrophic respiration" and "season∗" or "month∗" and "soil" or "land" or "terrestrial" on Google Scholar (http://scholar.google.com/) by September 2020. Similar to the procedure for MBC analysis, we only included full-year studies. Specifically, studies sampled at all seasons and included at least one measurement in each season, i.e., spring (March to May for the Northern Hemisphere and September to November for the Southern Hemisphere), summer (June to August for the Northern Hemisphere and December to February for the Southern Hemisphere), autumn (September to November for the Northern Hemisphere and March to May for the Southern Hemisphere), and winter (December to February for the Northern Hemisphere and June to August for the Southern Hemisphere). Raw values and units of Rh and available associated information such as the sampling date, and the latitude and longitude of the sampling site were recorded in the dataset. In total, we included 125 full-year seasonal variation measurements of Rh, with 2389 full-year data points from 56 articles (see Dataset and Tables S1, Supplementary Material). Since Rh was measured by different methods (e.g., root trenching, root removal, and gap analysis) from publications, the analysis using raw data may introduce uncertainties in the results. To reduce bias introduced by measurements in different studies, we conducted log-transformation following $Rh_{normalized} = \log_{10}(Rh_i/Rh_{mean})$ in which Rh_i indicates the Rh from each measurement, and Rh_{mean} is the annual average of Rh.

Data source of Rh in the CMIP6

We used soil temperature, moisture, litter, and SOM as model input data. Soil moisture and soil temperature at daily steps and litter and three SOM variables (i.e., SOM1, SOM2, and SOM3) at monthly steps during 1900 to 2014 were obtained from the model output by Community Earth System Model (CESM2.0) for Coupled Model Intercomparison Project (CMIP6), available at https://esgf-node.llnl.gov/search/cmip6/. Fifteen models from Coupled Model Intercomparison Project Phase 6 (CMIP6) were chosen for HR analysis. They are ACCESS-ESM1-5, BCC-CSM2-MR, BCC-ESM1, CanESM5, CESM2, CESM2-WACCM, CMCC-CM2-SR5, E3SM-1–1, E3SM-1–1-ECA, GFDL-ESM4, MPI-ESM-1–2-HAM, MPI-ESM1-2-LR, NorCPM1, NorESM2-LM, and TaiESM1 (Tables S1, Supplementary Material).

Monthly litter, SOM1, SOM2, and SOM3 were linearly interpolated to daily values using the "na.approx" function in R version 4.0.3 (54).

Land cover map for biome-level analysis

The global vegetation distribution dataset was obtained from a spatial map of 11 major biomes: boreal forest, temperate forest, tropical/subtropical forest, mixed forest, grassland, shrubland, tundra, desert, natural wetlands, cropland, and pasture, which have been used in our previous publications (55, 45, 3). The global land area database was from the surface data map of 0.5° × 0.5° generated for E3SM (https://web.lcrc.anl.gov/public/e3sm/inputdata/lnd/clm2/surfdata_map/).

Development of a semi-mechanistic model

We improved a semi-empirical modeling framework (10) that includes the fundamental processes in MBC accumulation to develop MBC seasonality (Fig. S2, Supplementary Material). The key processes include decomposition, carbon (C) assimilation, microbial growth and death, and microbial maintenance respiration (MMR). The decomposition of the substrate (D_c) is simulated as a function of substrate quality and microbial biomass stoichiometry, which is based on the carbon:nitrogen (C:N) ratio of substrate and microbial biomass (56, 57). The substrate in the model included a litter pool and three SOM pools (SOM1, SOM2, and SOM3). The classification of SOM pools was based on their turnover time, with a turnover time of 50 days, 5 years, and 222 years for SOM1, SOM2, and SOM3, respectively. Microbial C assimilation is controlled by CUE, which is described as a function of reference CUE (CUE_{ref}), temperature (T_{CUE}), reference temperature (T_{CUEref}) (63), microbial biomass stoichiometry (CN_B), and substrate quality (CN_{litter} and CN_{SOM}) (64)). The MMR was controlled by MBC, soil temperature, and soil moisture.

$$D_C = D_{litterC} + D_{SOMC}, \tag{1}$$

$$\frac{dMBC}{dt} = D_{litterC} \times CUE_{litter} + D_{SOMC} \times CUE_{SOM} - MMR - R_{lysis}, \tag{2}$$

$$D_{litterC} = C_{litter} \times k_{litter} \times f_s(T) \times f_s(M) \times \frac{MBC}{MBC + k_{es}}, \tag{3}$$

$$D_{SOMC} = (C_{SOM1} \times k_{SOM1} + C_{SOM2} \times k_{SOM2} + C_{SOM3} \times k_{SOM3}) \times f_s(T) \times f_s(M) \times \frac{MBC}{MBC + k_{es}}, \tag{4}$$

$$k_{litter} = \frac{1}{\tau_{litter}}, \tag{5}$$

$$k_{SOM1} = \frac{1}{\tau_{SOM1}}, \tag{6}$$

$$k_{SOM2} = \frac{1}{365 \times \tau_{SOM2}}, \tag{7}$$

$$k_{SOM3} = \frac{1}{365 \times \tau_{SOM3}}, \tag{8}$$

$$MMR = MBC \times k_m \times f_m(T) \times f_m(M), \tag{9}$$

$$R_{lysis} = MBC \times k_{lysis} \times f_m(T) \times f_m(M), \tag{10}$$

$$CUE_{litter} = (CUE_{ref} - (CUE_T \times (T - T_{CUEref}))) \times \left(\frac{CN_B}{CN_{litter}}\right)^{0.6}, \tag{11}$$

$$CUE_{SOM} = (CUE_{ref} - (CUE_T \times (T - T_{CUEref}))) \times \left(\frac{CN_B}{CN_{SOM}}\right)^{0.6}, \tag{12}$$

$$f_s(T) = Q_{10s}^{\frac{T - Ts_{ref}}{10}}, \tag{13}$$

$$f_m(T) = Q_{10m}^{\frac{T - Tm_{ref}}{10}}, \tag{14}$$

$$f_s(M) = \frac{\log\left(\frac{Ms_{min}}{M}\right)}{\log\left(\frac{Ms_{min}}{Ms_{max}}\right)}, \tag{15}$$

$$f_m(M) = \frac{\log\left(\frac{Mm_{min}}{M}\right)}{\log\left(\frac{Mm_{min}}{Mm_{max}}\right)}, \tag{16}$$

where D_c is the rate of substrate breakdown; $D_{litterC}$ is the rate of litter breakdown; D_{SOMC} is the rate of SOM breakdown; C_{litter} is the concentration of litter pool C; C_{SOM1} is the concentration of SOM pool 1 C; C_{SOM2} is the concentration of SOM pool 2 C; C_{SOM3} is the concentration of SOM pool 3 C; k_{litter} is the potential rate of litter breakdown; k_{SOM1} is the potential rate of SOM pool 1 breakdown; k_{SOM2} is the potential rate of SOM pool 2 breakdown; k_{SOM3} is the potential rate of SOM pool 3 breakdown; τ_{litter}, τ_{SOM1}, τ_{SOM2}, and τ_{SOM3} are turnover time of litter (20 days), SOM pool 1 (50 days), SOM pool 2 (5 years), and SOM pool 3 (222 years). $f_s(T)$ is the temperature effects on substrate breakdown, and $f_s(M)$ is the moisture effects on substrate breakdown; $f_m(T)$ is the temperature effects on microbial turnover, and $f_m(M)$ is the moisture effects on microbial turnover; MBC is the soil microbial biomass C; R_{lysis} is C loss through the microbial lysis, and k_{lysis} is the potential rate of microbial lysis; k_{es} is the half saturation constant for microbial effects on substrate breakdown; k_m is the potential C loss rate of microbial biomass through MMR; CUE_{ref} is the CUE at reference temperature; CUE_{litter} is the CUE of litter; CUE_{SOM} is the CUE of SOM; T_{CUEref} means the reference temperature for CUE (15°C); Ts_{ref} means the reference temperature for substrate decomposition (10°C); Tm_{ref} means the reference temperature for microbial biomass decomposition (12°C); Ms_{min} is the minimum moisture for substrate breakdown; Ms_{max} is the maximum moisture for substrate breakdown, moisture effect will be 1 if moisture is larger than Ms_{max}; CN_{litter} is the C:N ratio of litter; CN_{SOM} is the C:N ratio of SOM; CN_B is the C:N ratio of microbial biomass. The model has a daily time step.

Model application

The semi-mechanistic model developed for theoretical analysis of MBC seasonal dynamics was further applied to simulate the MBC variation at seasonal scale. Subsequent data analyses are based on steady-state simulations. All simulations run in total 41,975 days with top 30 cm soil temperature and soil moisture, litter, and whole-soil *SOM1*, *SOM2*, and *SOM3* of 115 years (1900 to 2014) as input data. Most simulations reach steady state in approximately 1095 days (Fig. S3, Supplementary Material). Long-term simulations were used to ensure steady state and consistency among simulations for latitudinal zones and sites. The model was first initialized with the parameters in Supplementary Table S2 and input data of daily soil temperature, soil moisture, *SOM1*, *SOM2*, and *SOM3* during 1900 to 2014. Daily MBC simulated by the theoretical model was computed as the monthly arithmetic mean of MBC during 2005 to 2014. Then, the monthly MBC was normalized following the equation of $Normalized\ MBC = log_{10}(\frac{MBC_i}{MBC_{mean}})$, in which MBC_i indicates the MBC in each month, and MBC_{mean} is the annual average of MBC. Next, we compared the monthly normalized simulated MBC with the observed MBC. The optimal values for CUE_{ref} and Q_{m10} of three latitudinal zones (0°N to 25°N, 25°N to 50°N, and 50°N to 90°N) were selected based on the model efficacy estimates, i.e., small MAE and RMSE and high R^2 values (Fig. S4, Supplementary Material).

Due to the temperature dependence of CUE and Q_{10} values, we tested the relationships between long-term soil temperature of three latitudinal zones (0°N to 25°N, 25°N to 50°N, and 50°N to 90°N) and CUE_{ref} and Q_{m10} values. We found high consistency between long-term soil temperature of three latitudinal zones (0°N to 25°N, 25°N to 50°N, and 50°N to 90°N) and their optimal CUE_{ref} ($R^2 = 0.996$) and Q_{m10} ($R^2 = 0.957$) values. Therefore, evident temperature dependence of CUE_{ref} and Q_{m10} exists (58, 59). For global simulation, the parameters of CUE_{ref} and Q_{m10} of each site were obtained based on long-term site soil temperature and well-established relationship between long-term site soil temperature and CUE_{ref} and Q_{m10} in three latitudinal zones (0°N to 25°N, 25°N to 50°N, and 50°N to 90°N).

Mapping global soil MBC at a monthly scale

We estimated the global distribution of MBC relative changes at a monthly scale based on the semi-mechanistic model developed in the previous section. In addition, soil MBC in Xu et al. (3) was estimated based on the long-term average of soil organic C concentration and climate conditions (e.g., precipitation), which can serve as the global long-term average of MBC. Therefore, the combined use of the empirical model in each month and soil MBC in Xu et al. (3) provides a feasible way to globally estimate MBC in each month. Based on the global soil MBC dataset in Xu et al. (3) and the global map of relative change in MBC in each month, we generated the global maps of monthly MBC (Fig. 2).

We then investigated the modeling performance of MBC by comparing the model simulation and observed data in each month (Fig. S5, Supplementary Material). We found the overall consistency between simulated and observed log-scaled MBC, indicating the robustness of the empirical models in estimating the seasonal variation of MBC. However, it is noteworthy that the modeling efficacy was untested in the Southern Hemisphere and managed biomes (e.g., cropland and pasture), attention needs to be paid when interpreting the MBC in the Southern Hemisphere and managed biomes.

Uncertainty analysis

To estimate the parameter-induced uncertainties in MBC distribution and storage, we used the improved Latin Hypercube Sampling (LHS) approach to estimate the parameter-led uncertainty in MBC at both biome and global scales. The LHS approach can randomly produce an ensemble of parameter combinations with high efficiency. This approach has been widely used in the modeling community to estimate uncertainties in the model output (60, 61, 10). We first assumed that all parameters follow a normal distribution, and then used LHS to randomly select an ensemble of 1000 parameter sets using the function of "improved LHS" in the R package "lhs" (62).

Data source for diagram development

To better understand the controls on the four phases of MBC (i.e., valley, increasing, peak, and declining), we chose regions with the most distinguished four-phase pattern in low-, mid- and high-latitude regions for analysis. In specific, we included data from 70° to 80° in the high latitudes, 40° to 50° in the mid-latitudes, and 10° to 20° in the low latitudes in Northern Hemisphere. For phase 1 (valley phase), we chose data from May, June, and July in the low latitudes, August and September in the mid-latitudes, and September and October in the high latitudes. For phase 2 (climbing phase), data from August, September, October, November, and December in the low latitudes, October, November, and December, January, and February in the mid-latitudes, and January, February, March, October, November, and December in the high latitudes were chosen. For phase 3 (peak phase), we chose data from January and February in the low latitudes, March and April in the mid-latitudes, and April, May, and June in the high latitudes. For phase 4 (declining phase), we included data from March and April in the low latitudes, May, June, and July in the mid-latitudes, and July and August in the high latitudes. We then randomly selected 100 data pairs of substrates (decomposed carbon

from litter and three SOM pools in the semi-mechanistic model), ST, and SM in each phase, and 1200 data pairs in total were included for generalized linear analysis to attribute variations in MBC.

Standard deviation

We calculated the arithmetic mean microbial biomass ($\bar{x}$) and SD for each month and each quarter. Meanwhile, to describe the MBC seasonality shifts along latitude, we also calculated the mean microbial biomass ($\bar{x}$) and SD at low (0°N–25°N), mid- (25°N~50°N), and high latitudes (>50°N) for each month. The SDs were used to represent the spatial variation of microbial biomass among the sampling points, where x_i indicates the MBC in each month or quarter; n is the number of data points for caltulation.

$$SD = \sqrt{SD^2} = \sqrt{\frac{\sum_{i=1}^{n}(x_i - \bar{x})^2}{n-1}}. \quad (17)$$

Statistical analysis

We applied the log-transformation to normalize the microbial biomass data to be consistent in seasonality across sites (Fig. S1, Supplementary Material). We performed a normality test using the Shapiro–Wilk test. The log-transformation was adopted as it was the best to normalize the data for robust statistical analysis (Fig. 1). All statistical analyses were conducted using the R program version 3.5.3 (54); all figures displayed in this study (except for Fig. 2 made using ArcGIS 10.1) were generated using Origin 8.5 and the R program version 3.5.3 (54).

Acknowledgments

The authors are grateful to the editor and three anonymous reviewers for their constructive comments that have substantially improved the manuscript.

Supplementary Material

Supplementary material is available at *PNAS Nexus* online.

Funding

X.X. and L.H. were supported by the US National Science Foundation (2145130 to X.X.), San Diego State University, and the CSU Program for Education and Research in Biotechnology. This work was financially supported by the National Science Foundation of China (42277284 to F.Z.) and the 2021 first funds for the central government to guide local science and technology development in the Qinghai Province (No. 2021ZY002 to F.Z.).

Authors' Contributions

X.X. conceived the project. F.Z. compiled all data of microbial biomass data for seasonal variation. L.H. performed modeling analysis. J.W., G.P., and W.U. contributed to data visualization. All authors interpreted the results and wrote the manuscript.

Code Availability

The code for data analysis and global mapping for microbial residence time can be accessed at https://github.com/email-lhe/MBCdyn_fig_code.

Data Availability

The data used for analysis in this study are documented in the "Materials and methods" section or in the Supplementary Material. All data used for analysis are archived at https://doi.org/10.5061/dryad.hdr7sqvmt.

References

1. Gougoulias C, Clark JM, Shaw LJ. 2014. The role of soil microbes in the global carbon cycle: tracking the below-ground microbial processing of plant-derived carbon for manipulating carbon dynamics in agricultural systems. J Sci Food Agric. 94: 2362–2371.
2. Singh BK, Bardgett RD, Smith P, Reay DS. 2010. Microorganisms and climate change: terrestrial feedbacks and mitigation options. Nat Rev Microbiol. 8: 779–790.
3. Xu X, Thornton PE, Post WM. 2013. A global analysis of soil microbial biomass carbon, nitrogen and phosphorus in terrestrial ecosystems. Glob Ecol Biogeogr. 22: 737–749.
4. Li Y, Xu M, Zou X. 2006. Heterotrophic soil respiration in relation to environmental factors and microbial biomass in two wet tropical forests. Plant Soil. 281: 193–201.
5. Wang WJ, Dalal RC, Moody PW, Smith CJ. 2003. Relationships of soil respiration to microbial biomass, substrate availability and clay content. Soil Biol Biochem. 35: 273–284.
6. Ataka M, Kominami Y, Sato K, Yoshimura K. 2020. Microbial biomass drives seasonal hysteresis in litter heterotrophic respiration in relation to temperature in a warm-temperate forest. J Geophys Res Biogeosci. 125: e2020JG005729.
7. Schimel JP, Schaeffer SM. 2012. Microbial control over carbon cycling in soil. Front Microbiol. 3: 1–11.
8. Walker TW, *et al.* 2018. Microbial temperature sensitivity and biomass change explain soil carbon loss with warming. Nat Clim Chang. 8: 885–889.
9. Wieder WR, *et al.* 2015. Explicitly representing soil microbial processes in Earth system models. Glob Biogeochem Cycles. 29: 1781–1800.
10. Xu X, *et al.* 2014. Substrate and environmental controls on microbial assimilation of soil organic carbon: a framework for Earth system models. Ecol Lett. 17: 547–555.
11. Lin B, Zhao X, Zheng Y, Qi S, Liu X. 2017. Effect of grazing intensity on protozoan community, microbial biomass, and enzyme activity in an alpine meadow on the Tibetan Plateau. J Soils Sediments. 17: 2752–2762.
12. Lu XY, Fan JH, Yan Y, Wang XD. 2013. Comparison of soil microbial biomass and enzyme activities among three alpine grassland types in Northern Tibet. Pol J Environ Stud. 22: 437–443.
13. Wei H, *et al.* 2015. Are variations in heterotrophic soil respiration related to changes in substrate availability and microbial biomass carbon in the subtropical forests? Sci Rep. 5: 18370.
14. Birge HE, *et al.* 2015. Soil respiration is not limited by reductions in microbial biomass during long-term soil incubations. Soil Biol Biochem. 81: 304–310.
15. Wardle DA. 1998. Controls of temporal variability of the soil microbial biomass: a global-scale synthesis. Soil Biol Biochem. 30: 1627–1637.
16. Díaz-Raviña M, Acea MJ, Carballas T. 1995. Seasonal changes in microbial biomass and nutrient flush in forest soils. Biol Fertil Soils. 19: 220–226.
17. Cochran VL, Elliott LF, Lewis CE. 1989. Soil microbial biomass and enzyme activity in subarctic agricultural and forest soils. Biol Fertil Soils. 7: 283–288.

18. Edwards KA, Jefferies RL. 2013. Inter-annual and seasonal dynamics of soil microbial biomass and nutrients in wet and dry low-Arctic sedge meadows. Soil Biol Biochem. 57: 83–90.
19. Jin V, Schaeffer S, Ziegler S, Evans R. 2011. Soil water availability and microsite mediate fungal and bacterial phospholipid fatty acid biomarker abundances in Mojave Desert soils exposed to elevated atmospheric CO_2. J Geophys Res Biogeosci. 116:G02001.
20. Feng W, Zou X, Schaefer D. 2009. Above- and belowground carbon inputs affect seasonal variations of soil microbial biomass in a subtropical monsoon forest of southwest China. Soil Biol Biochem. 41: 978–983.
21. Konings AG, *et al.* 2019. Global satellite-driven estimates of heterotrophic respiration. Biogeosciences. 16: 2269–2284.
22. He L, *et al.* 2021. Dynamics of fungal and bacterial biomass carbon in natural ecosystems: site-level applications of the CLM-microbe model. J Adv Model Earth Syst. 13: e2020MS002283.
23. Rousk J, Bååth E. 2007. Fungal and bacterial growth in soil with plant materials of different C/N ratios. FEMS Microb Ecol. 62: 258–267.
24. Rousk J, Brookes PC, Bååth E. 2009. Contrasting soil pH effects on fungal and bacterial growth suggest functional redundancy in carbon mineralization. Appl Environ Microbiol. 75: 1589–1596.
25. Lipson DA, Schmidt SK, Monson RK. 2000. Carbon availability and temperature control the post-snowmelt decline in alpine soil microbial biomass. Soil Biol Biochem. 32: 441–448.
26. Griffiths BS. 1994. Microbial-feeding nematodes and protozoa in soil: their effectson microbial activity and nitrogen mineralization in decomposition hotspots and the rhizosphere. Plant Soil. 164: 25–33.
27. Kooch Y, Noghre N. 2020. The effect of shrubland and grassland vegetation types on soil fauna and flora activities in a mountainous semi-arid landscape of Iran. Sci Total Environ. 703: 135497.
28. Kuzyakov Y, Xu X. 2013. Competition between roots and microorganisms for nitrogen: mechanisms and ecological relevance. New Phytol. 198: 656–669.
29. Xu X, Ouyang H, Richter A, Wanek W, Cao G, Kuzyakov Y. 2011. Spatio-temporal variations determine plant–microbe competition for inorganic nitrogen in an alpine meadow. J Ecol. 99: 563–571.
30. Bahram M, *et al.* 2018. Structure and function of the global topsoil microbiome. Nature. 560: 233.
31. Wang Q, *et al.* 2021. Differences in root exudate inputs and rhizosphere effects on soil N transformation between deciduous and evergreen trees. Plant Soil. 458: 277–289.
32. Hannula SE, *et al.* 2019. Time after time: temporal variation in the effects of grass and forb species on soil bacterial and fungal communities. mBio. 10: e02635–e02619.
33. Griffiths RI, Whiteley AS, O'Donnell AG, Bailey MJ. 2003. Influence of depth and sampling time on bacterial community structure in an upland grassland soil. FEMS Microbiol Ecol. 43: 35–43.
34. Stevenson B A, Hunter DWF, Rhodes PL. 2014. Temporal and seasonal change in microbial community structure of an undisturbed, disturbed, and carbon-amended pasture soil. Soil Biol Biochem. 75: 175–185.
35. Lipson DA, Schadt CW, Schmidt SK. 2002. Changes in soil microbial community structure and function in an alpine dry meadow following spring snow melt. Microb Ecol. 43: 307–314.
36. He L, Xu X. 2021. Mapping soil microbial residence time at the global scale. Glob Chang Biol. 27: 6484–6497.
37. Vancampenhout K, *et al.* 2009. Differences in chemical composition of soil organic matter in natural ecosystems from different climatic regions—a pyrolysis—GC/MS study. Soil Biol Biochem. 41: 568–579.
38. Takriti M, *et al.* 2018. Soil organic matter quality exerts a stronger control than stoichiometry on microbial substrate use efficiency along a latitudinal transect. Soil Biol Biochem. 121: 212–220.
39. Bell CW, Acosta-Martinez V, McIntyre NE, Cox S, Tissue DT, Zak JC. 2009. Linking microbial community structure and function to seasonal differences in soil moisture and temperature in a Chihuahuan desert grassland. Microb Ecol. 58: 827–842.
40. Rasche F, *et al.* 2011. Seasonality and resource availability control bacterial and archaeal communities in soils of a temperate beech forest. ISME J. 5: 389–402.
41. Zhong ZK, *et al.* 2020. Adaptive pathways of soil microorganisms to stoichiometric imbalances regulate microbial respiration following afforestation in the Loess Plateau, China. Soil Biol Biochem. 151: 108048.
42. Sinsabaugh RL, *et al.* 2016. Stoichiometry of microbial carbon use efficiency in soils. Ecol Monogr. 86: 172–189.
43. Blagodatsky SA, Heinemeyer O, Richter J. 2000. Estimating the active and total soil microbial biomass by kinetic respiration analysis. Biol Fertil Soils. 32: 73–81.
44. Pietikäinen J, Pettersson M, Bååth E. 2005. Comparison of temperature effects on soil respiration and bacterial and fungal growth rates. FEMS Microbiol Ecol. 52: 49–58.
45. Xu X, *et al.* 2017. Global pattern and controls of soil microbial metabolic quotient. Ecol Monogr. 87: 429–441.
46. Wang G, *et al.* 2022. Soil enzymes as indicators of soil function: a step toward greater realism in microbial ecological modeling. Glob Chang Biol. 28: 1935–1950.
47. Wang G, *et al.* 2015. Microbial dormancy improves development and experimental validation of ecosystem model. ISME J. 9: 226–237.
48. Brown R, Markewitz D. 2018. Soil heterotrophic respiration: measuring and modeling seasonal variation and silvicultural impacts. For Ecol Manag. 430: 594–608.
49. Capek P, Starke R, Hofmockel KS, Bond-Lamberty B, Hess N. 2019. Apparent temperature sensitivity of soil respiration can result from temperature driven changes in microbial biomass. Soil Biol Biochem. 135:286–293.
50. Bittman S, Forge T, Kowalenko C. 2005. Responses of the bacterial and fungal biomass in a grassland soil to multi-year applications of dairy manure slurry and fertilizer. Soil Biol Biochem. 37: 613–623.
51. Kaiser C, *et al.* 2010. Belowground carbon allocation by trees drives seasonal patterns of extracellular enzyme activities by altering microbial community composition in a beech forest soil. New Phytol. 187: 843–858.
52. Buchkowski RW, Shaw AN, Sihi D, Smith GR, Keiser AD. 2019. Constraining carbon and nutrient flows in soil with ecological stoichiometry. Front Ecol Evol. 7:382.
53. Spohn M. 2016. Element cycling as driven by stoichiometric homeostasis of soil microorganisms. Basic Appl Ecol. 17: 471–478.
54. R. R Core Team 2020. R: A language and environment for statistical computing. Vienna, Austria: R Foundation for Statistical Computing. URL: https://www.r-project.org
55. Guo Z, *et al.* 2020. Soil dissolved organic carbon in terrestrial ecosystems: global budget, spatial distribution and controls. Glob Ecol Biogeogr.29:2159–2175.
56. Schimel JP, Weintraub MN. 2003. The implications of exoenzyme activity on microbial carbon and nitrogen limitation in soil: a theoretical model. Soil Biol Biochem. 35: 549–563.
57. Zhang D, Hui D, Luo Y, Zhou G. 2008. Rates of litter decomposition in terrestrial ecosystems: global patterns and controlling factors. J Plant Ecol. 1: 85–93.

58. Hamdi S, Moyano F, Sall S, Bernoux M, Chevallier T. 2013. Synthesis analysis of the temperature sensitivity of soil respiration from laboratory studies in relation to incubation methods and soil conditions. Soil Biol Biochem. 58: 115–126.
59. Pold G, Domeignoz-Horta LA, Morrison EW, Frey SD, Sistla SA, DeAngelis KM. 2020. Carbon use efficiency and its temperature sensitivity covary in soil bacteria. MBIO. 11:e02293–19.
60. Haefner JW. 2005. Modeling biological systems-principles and applications. New York (NY):Springer.
61. Xu X. 2010. Modeling methane and nitrous oxide exchanges between the atmosphere and terrestrial ecosystems over North America in the context of multifactor global change. [Dissertation]. Auburn (AL): Auburn University.
62. Carnell R. 2020. lhs: Latin Hypercube Samples, R package version 1.0.2, [accessed on 20 October 2021]available at https://CRAN.R-project.org/package=lhs
63 Allison Steven D, Matthew Wallenstein D, Bradford Mark A. 2010. Soil-carbon response to warming dependent on microbial physiology. Nat Geosci. 3(5):336–340
64 Manzoni Stefano, Jackson Robert B, Trofymow John A, Porporato Amilcare. 2008. The Global Stoichiometry of Litter Nitrogen Mineralization. Science. 321(5889):684–686